

## **INFLUENCE OF BLENDED CEMENT WITH HCFA ON MICROSTRUCTURE AND CHLORIDE IONS TRANSPORT OF CONCRETE RESISTANT TO SURFACE SCALING**

Mariusz DĄBROWSKI<sup>1</sup>, Karolina GIBAS, Michał A. GLINICKI  
Institute of Fundamental Technological Research Polish Academy of Sciences  
5B, Pawińskiego Str., 02-106 Warszawa, Poland, <sup>1</sup>e-mail: mdabrow@ippt.pan.pl

### **ABSTRACT**

The relationship between the internal pore characteristic and the non-steady state chloride migration coefficient ( $D_{nssm}$ ) was investigated for concrete mixes made with blended cement containing high calcium fly ash (HCFA). Air entrained concrete mixes were made using granodiorite and crushed limestone as coarse aggregate. Designed surface scaling resistance was confirmed with standard test. The pore structure was determined using mercury intrusion porosimetry (MIP) and digital image analysis techniques. Phase composition of hydration products was examined using the XRD analysis. Chloride ion transport velocity was measured using a rapid chloride migration test. The test has shown a relationship between the chloride migration coefficient and pore size characteristic derived from MIP tests. Effect of aggregate type on the course of relationship as shown differences curve for both type of aggregates. Increase amount of additives in blended cements caused decrease of critical and average pore size obtained by MIP method.

### **Keywords**

HCFA, blended cement, chloride ions migration, MIP, scaling resistance

### **INTRODUCTION**

The application of air-entraining admixtures is the most common method to ensure the frost resistance and scaling resistance of concrete. From the ecological and economical point of view the growing use of mineral admixtures to cement and concrete technology is beneficial but the supplementary cementitious materials (SCM) strongly influence the effectiveness of air-entraining admixtures. The proper use of the air entrainment admixtures is a process highly sensitive to fineness and unburned carbon content of fly ash [1-3]. Thus properties of common used SCMs are controlled very precisely in order to limit technological problems on construction site.

Calcareous fly ash is one of coal combustion products, which could be used in cement and concrete technology. Positive experiences with HCFA utilization in concrete presented in USA and Canada caused discussion about use of its domestic resources. There are several restrictions on use of this kind of fly ash in cement industry. One of them is a large variability of physical properties and chemical composition of HCFA, which causing disagreement with current European standards [4]. However, a positive potential of HCFA as a cement additive was presented by many researchers [5-6] especially in relation to strength and liquid transport properties [7-8].

The use of air-entraining admixture in concrete mix is aimed to provide additional porosity which are fine air bubbles uniformly distributed throughout concrete, spaced densely

enough to enable accommodation of stresses resulting from the increase of volume of water in the capillary pores during freezing. Wong et al. [9] in his research conclude that air voids from air-entraining process have no impact on rate of fluid and liquid transport. It follows that the transport rate of liquid in frost resistance concrete depends only on permeability of cement matrix.

Presented short review indicated that HCFA could be a valuable constituent of blended cements especially when the reduction of ion transport into concrete is expected. Thus the purpose of the current research is to evaluate the effect of HCFA and synergy of this kind of additive with low calcium fly ash (FA) or ground granulated blast furnace slag (GGBS) used in blended cements on the microstructure and moisture transport properties of air-entrained concrete.

## EXPERIMENTAL PROGRAM

### Materials using to create blended cements

Manufacturing of new blended cements with using of HCFA was performed out after a complex investigation of physical and chemical properties of such waste material from Bełchatów Power Plant. After that were selected one of them then assigned to creation experimental cements. Other additional materials were selected with a view to common popular waste material used in blended cements in Poland. Chemical composition selected materials used to produce blended cements are presented in Table 1. Portland clinker, siliceous fly ash (FA) and ground granulated blast furnace slag (GGBS) contain typical amount of oxides for this type of addition materials, in compliance to European standards. Morphology of HCFA was presented at Fig.1. Part of HCFA grains are perfectly round which indicates a presence of amorphous phases. A significant part of grains are irregular and have rough texture (Fig.1 b1). This image is representative for clay minerals which lost chemically bond water by ignition in power plant boiler. Were observed also grains of unburned coal (Fig.1 b2).

Cements were produced by collected grinding to a designed Blaine surface area, close to ordinary cement. Addition of gypsum was adjusted to the proportioned total content of  $\text{SO}_3$  ion in composition of cements. Designation of cement type was consistent with European Standards except CEM V, due to absence of HCFA addition in this type of cement. Details of blended cement composition and physical properties are shown in Table 2.

### Concrete mix composition

New cements were used in concrete mixtures proportioned according to European standards concerning the most drastic environmental condition related to freeze and thaw cycles and deicing chemicals exposure. The reference concrete with ordinary cement content  $340\text{kg/m}^3$  was prepared with water to cement ratio  $w/c=0.45$ . The choice of aggregates resulted in the selection of two different types of aggregates. Granodiorite is the igneous rock typical for frost resistant concrete whereas limestone aggregates is sedimentary rock where  $\text{CaCO}_3$  is the main mineral. The main difference between both kinds of rocks is texture of grain surface that result in different properties of interfacial transition zone (ITZ) [10].

Selection of proper dosage of chemical admixtures was a very important part of technological work. At first an air-entraining admixture (AEA) was applied to achieve the target total volume of entrained air at 6-7% tested by pressure method. When a proper volume of air in concrete mixture was achieved the next step was an addition of a superplasticizer (SP) until the slump was in the range 50-100mm. At this case possible was next dosage of

superplasticizer when slump measurement was less than 50mm. Concrete mixture composition is shown in Table 3.

Specimens were cured for 90 days in water, after that were subjected to planned tests.

Table 1. Chemical composition of clinker and other major components of HCFA blended cements (XRF analysis;  $\text{CaO}_f$  – glycol method; LOI – oven up to  $1000^\circ\text{C}$ ;  $\text{SO}_3$  – elemental analysis method) [11]

Component [%]										
	CaO	SiO <sub>2</sub>	Al <sub>2</sub> O <sub>3</sub>	Fe <sub>2</sub> O <sub>3</sub>	MgO	SO <sub>3</sub>	K <sub>2</sub> O	Na <sub>2</sub> O	CaO <sub>f</sub>	LOI
Portland clinker	66.7	22.7	4.9	2.4	1.0	0.4	0.39	0.42	-	0.4
HCFA	26.0	40.9	19.0	4.3	1.7	3.9	0.14	0.13	1.07	2.1
FA	3.4	52.3	27.5	6.2	2.7	0.4	1.2	3.30	-	1.9
Slag	45.6	37.0	6.8	1.6	5.5	1.2	0.1	0.50	-	0.7

Table 2. The composition and physical properties of blended cements

Cement type	Portland clinker [%]	HCFA [%]	FA [%]	Slag [%]	Gypsum [%]	Surface area (Blaine) [cm <sup>2</sup> /g]	SO <sub>3</sub> content by mass [%]
CEM I	95	-	-	-	5	3900	2.8
CEM II/B-W	66	39	-	-	4	3800	3.1
CEM II/B-M (V-W)	65	14	14	-	5	3800	3.1
„CEM V/A (S-W)”	48	24	-	24	4	3800	3.3

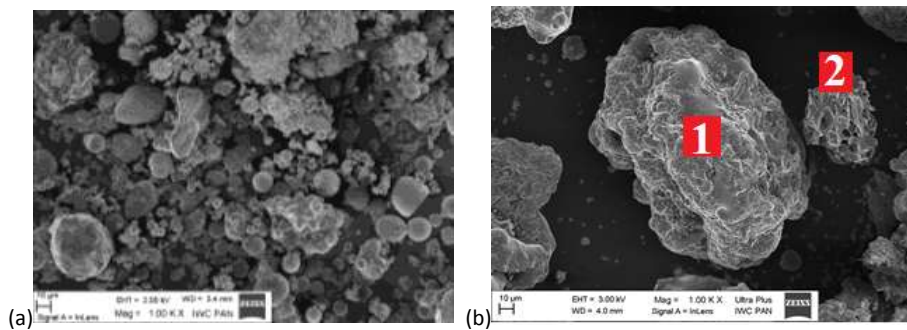


Fig. 1. Selected SEM micrographs: (a) example of HCFA (b1) example grains  $> 125 \mu\text{m}$  (b2) unburned carbon

Table 3. Concrete mix design

Concrete mix	Cement type <sup>a)</sup>	Other constituents of concrete mix [kg/m <sup>3</sup> ]							
		Sand		Granodiorite		Limestone		Water	Admixtures
	0-2 mm	2-8 mm	8-16 mm	2-8 mm	8-16 mm	340 kg/m <sup>3</sup>	AEA		SP
GW-0	CEM I	598	607	602	-	-	153	0.22	0.2
GW-30	CEM II/B-W							0.69	0.9
GWV-30	CEM II/B-M (V-W)							0.41	0.5
GWS-50	„CEM V/A (S-W)”							0.52	1.0
LW-0	CEM I	605	-	-	625	578	153	0.18	0.4
LW-30	CEM II/B-W							0.76	1.2
LWV-30	CEM II/B-M (V-W)							0.38	1.7
LWS-50	„CEM V/A (S-W)”							0.66	1.3

<sup>a)</sup> type of new cement according to table 2

## METHODOLOGY AND TESTS PERFORMED

**Phasecomposition of cement paste** was examined using X-ray diffraction method. Test samples were dried at 40°C and powdered and sieved through a 0.045 mm sieve. Sieve residue was ground until entire powder was smaller than 45 µm. The TUR-M62 diffractometer was used with a voltage ratio of 40kV and 20mA lamp current. Copper lamp was used as an X-ray source. The scan step size was 0.05°, the collection time 5s, and in the range 2θ CuKα from 5° to 65°.

**Microstructure observation** was carried out using Zeiss-SUPRA SEM microscopy.

**Air void characteristic** in hardened concrete was determined using a computer-driven system of automatic image analysis. Tests were performed using polished concrete specimens 100x100x25 mm cut from cube specimens (150mm). The automatic measurement procedure was designed to comply with the requirements imposed by EN 480-11:2008. Results of measurements were available as a set of standard parameters for air void microstructure characterization: spacing factor – L [mm]; specific surface –  $\alpha$  [1/mm]; air content – A [%]; content of air voids with diameter less than 0.3 mm - A300 [%]. The test was conducted on two samples for each concrete mix.

**Mercury intrusion porosimetry (MIP)** test was performed on the small cores of concrete (Ø=16mm; h=25mm; weight≈ 9g) obtained from bars by drilling in concrete plates. Specimens were dried at 105°C for approximately until a constant weight was achieved and then they were kept in sealed containers until the day of the test. Quantachrome POREMASTER 60 mercury porosimeter was used, which could detect the pores as small as 5 nm with the maximum pressure of 414 MPa. The critical pore size was calculated as maximum of a derivative of MIP value.

**Surface scaling resistance test** was carried out with an automatic chamber for freezing and thawing of samples, using Slab test, according to *PKN-CEN/TS 12390-9: 2007 Testing hardened concrete – Part 9: Freeze-thaw resistance – Scaling*. For each series of concrete the test was conducted on three samples of 150×150×70mm, which were subjected to 56 freeze-

thaw cycles in the presence of 3% NaCl. To assess the resistance of concrete to scaling the criteria of the Swedish standard for Borås method SS 137244 were used.

**Rapid chloride migration test** was applied to the non-steady state migration coefficient according to Nordtest Method NT Build 492. The conformity criteria for concretes are based on the voltage magnitude, temperature of anolite measured on the beginning and end of test and the depth of chloride ions penetration. The non-steady-state migration coefficient ( $D_{nssm}$ ), is calculated from the Fick's second law. The following evaluation of the concrete resistance to chloride ions penetration was applied: from "very good" ( $D_{nssm} < 2 \times 10^{-12} \text{ m}^2/\text{s}$ ) to "unacceptable" ( $D_{nssm} > 16 \times 10^{-12} \text{ m}^2/\text{s}$ ). The test was conducted on three specimens for each concrete mix.

## RESULTS AND DISCUSSIONS

Figure 2 show differences between XRD reflection spectra for reference cement paste and cement paste made with 29% addition of HCFA. The intensity of portlandite reflex is the main difference between two types of cement paste. Probably it was caused by diluting of Portland clinker through SCM and was partially caused of pozzolanic reaction of HCFA during maturing time. Additionally on the XRD pattern the increase of intensity of ettringite reflex intensity is seen and new peaks from minerals included in HCFA are displayed (Fig.2d).

The spacing factor of air voids determine on hardened concrete was less than 0.20 mm (Fig.3b), the amount of micropores was far greater than 1.8% for all tested concretes. The parameters of air void microstructure were in accordance with the common requirements for concrete exposed to harsh environmental conditions associated with freezing and thawing (Fig.3a). The proper air entrainment of concrete confirm the results of scaling resistance test (Fig.4b). All tested concrete exhibit very good resistance to frost salt scaling. The measured mass of scaled material remains at very low level, hence comparison of each values are insignificant.

If the air void content and distribution is similar for all tested concretes then mechanical and physical properties of concrete can be largely attributed to the type of cement and aggregate used. Compressive strength values are shown in Figure 4a. Both reference concretes without SCM reached similar results near to 48 MPa. Concrete specimens made with blended cement achieved the highest compressive strength values. This effect confirms results presented in previous studies [4-5]. Possible explanation of this fact is the formation of denser microstructure of hydration products after 90 days of water curing related to pozzolanic reaction. A second possible explanation is associated with physical properties of HCFA. This kind of ash added to Portland clinker and co-milling to create blended cement cause increase of grain fineness. Hence more precisely filled spaces between aggregate requires less cement paste to create dense material.

The microstructure of capillary pores was characterized using three MIP parameters: the total pore volume (TPV), the critical pore diameter (CPD) and the average pore diameter (APD). The TPV for both types of aggregates were in the range 0.029-0.048  $\text{cm}^3/\text{g}$  (Table 4). However, these values are not good enough to describe tested materials because no information is given on the distribution of particular pore size. Therefore two other parameters are introduced. The first one CPD describe the critical pore size which constitute the most numerous group of capillary pores. The APD represents a value representative for a half of total porosity for each kind of concrete. Reference concretes with granodiorite and limestone aggregate are characterized by the highest value of CPD and APD compared to other concrete mixes. The results show a significant difference between these two indicators

for both reference concrete. More than four time increase of CPD for concrete with granodiorite aggregate was unexpected. The use of blended cement caused a decrease of CPD value for all made concretes. The nature of the reduction depends on the type of aggregate but differences between concrete mixes with the same cement type were not so significant.

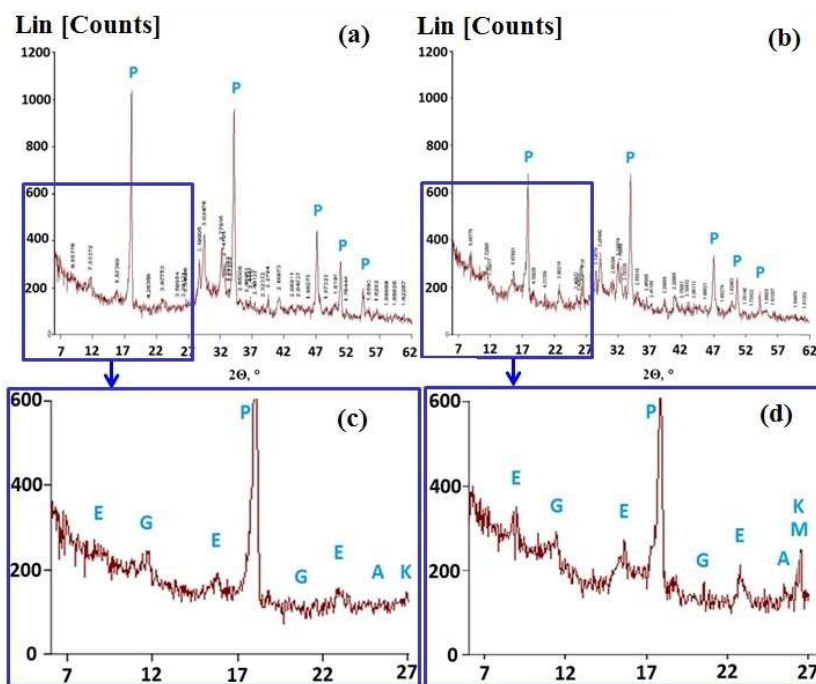


Fig.2. XRD pattern: (a) CEM I; (b) CEMII/B-W; (c)magnification of CEM I spectra; (d) magnification of CEMII/B-W spectra (P-portlandite; G-gypsum; E-ettringite; K-quartz; A-anhydrite; M-mullite)

For tested concrete compositions results of  $D_{nssm}$  are presented in Table 4. Obtained values of  $D_{nssm}$  reveal a positive impact of HCFA and other additives on the reduction of ions ingress into concrete. This observation confirm conclusions of other researchers [12-13] about an improve of transport properties concretes made with cements containing HCFA. These of bended cements with mixture of HCFA and other additives provide more impermeable cement matrix than with cement containing only HCFA. The values of  $D_{nssm}$  for concrete with reference cement was classified to “acceptable” class of chloride resistance, whereas all of concrete with blended cement obtain “good” class of impermeability according to Tang classification [14]. This issue was widely discussed in Aponte et al. [13] study, where influence of aggregate type on  $D_{nssm}$  was also observed. Concrete made with limestone aggregate and blended cement achieved the smallest  $D_{nssm}$  in comparison with concrete their corresponding concrete with granodiorite aggregate. Only for concrete made with cement with HCFA the opposite effect was observed.

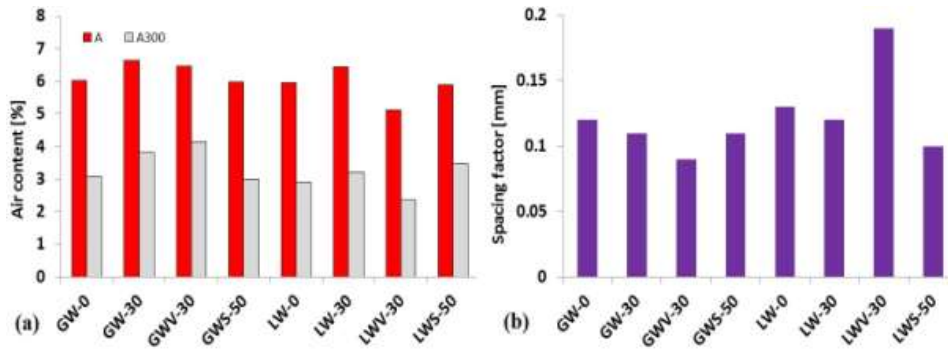


Fig.3. Quantitative characteristics of air voids in hardened concrete: (a) A- the total volume of air voids and A<sub>300</sub> – the content of micropores; (b)  $\bar{L}$  - the spacing factor)

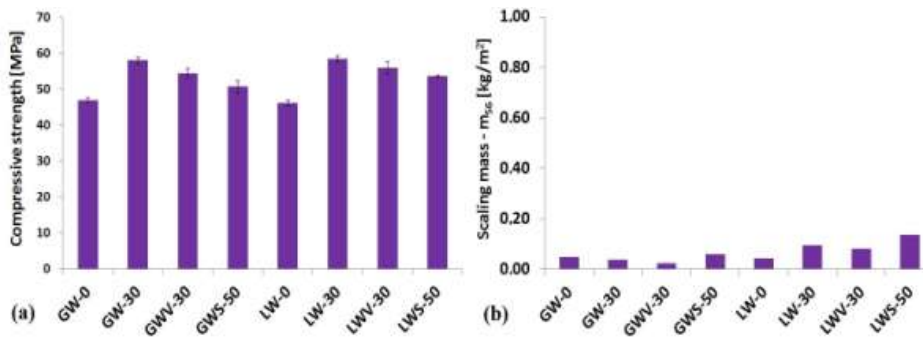


Fig. 4. Properties of concrete mixes after 90 days of water curing: (a) compressive strength; (b) mass of scaled material after exposure to freeze-thaw cycles according to PKN-CEN/TS 12390-9

Table 4. Results of MIP measurement

Concrete series	G W-0	G W-30	G WV-30	G WS-50	L W-0	L W-30	L WV-30	L WS-50
TPV [cm <sup>3</sup> /g]	0.048	0.038	0.029	0.041	0.035	0.046	0.031	0.030
CPD [nm]	463	71	89	44	99	77	57	47
APD[nm]	402	96	103	49	139	112	60	64
Average D <sub>nssm</sub> [x10 <sup>-12</sup> m <sup>2</sup> /s]	9.93	4.18	4.34	3.63	7.90	6.05	2.63	2.61
Standard deviation of D <sub>nssm</sub>	2.05	0.68	0.79	1.72	0.70	1.48	2.09	1.21

The most important findings of current study concern the relationship between the resistance of concretes with blended cements to chloride penetration and their microstructure parameters. Yang [15] obtains a linear relationship between the total pore volume measured by MIP test

and the chloride ingress into concrete measured by rapid method in non-steady and steady state. In that case the change of porosity was regulated by w/c ratio. Within the current investigation changes of porosity were obtained using blended cement with SCM and the same w/c ratio for all mixtures (w/c=0.45). Minerals additives caused qualitative and quantitative changes of hydration products in hardened concrete. Fig. 5 shows the absence of any relationship between  $D_{nssm}$  and TPV. However, the remaining MIP parameters (CPD and APD) are found more appropriate to draw a linear relationship like the one shown in Fig. 6. Microstructural changes of cement paste have a significant impact on the degree of cement matrix permeability, what confirm Leman et al. [16] observation for concretes made with blended cement. Hence was assumed that only the properties of cement paste have impact on  $D_{nssm}$ . Granodiorite aggregate has slightly less impact on  $D_{nssm}$  changes than limestone aggregate. It is evident, that an increase of pore size index causes an increase of  $D_{nssm}$ .

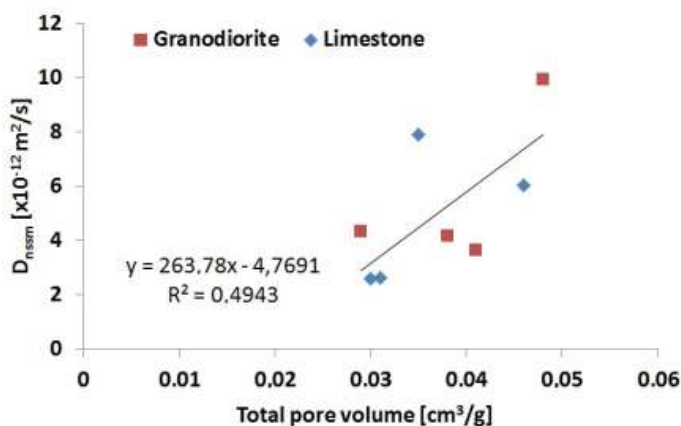


Fig. 5. Relationship between chloride migration coefficient ( $D_{nssm}$ ) and total pore volume (TPV)

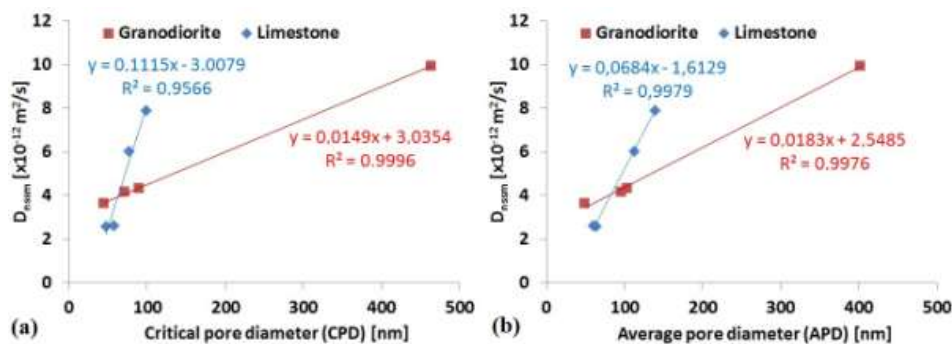


Fig. 6. Chloride migration coefficient ( $D_{nssm}$ ) versus: (a) critical pore diameter (CPD); (b) average pore diameter (APD)



## CONCLUSIONS

On the basis of results obtained in this investigation, the following concluding remarks are derived:

- Proper execution of air entraining process provides a stable microstructure of air voids necessary to obtain surface scaling resistance concrete with blended cements. Proportional to the amount of HCFA in blended cements increase amount of AEA necessary to achieve the same level of air voids volume.
- After 90 days of water curing concrete with blended cement achieved the compressive strength value from 5% to 20% higher than the reference concrete with Portland cement. No significant strength differences were found for concretes with the same kind of blended cement and different types of aggregate.
- The mass of scaled material resulting from freeze-thaw testing with the presence of de-icing salts remained at a very low level, especially for concrete with blended cement and granodiorite aggregates.
- Modification of Portland cement due to the use 30% of HCFA as additives leads to quantitative differences in the phase composition of cement matrix. The portlandite content decrease was proportional to a clinker replacement rate by HCFA.
- The reduction of  $D_{nssm}$  was proportional to increase of SCM in cement composition. The smallest value  $D_{nssm}$  was obtained for concretes with limestone aggregate and ternary cements, approximately three times lowest than for the reference concrete.
- The capillary pore microstructure analysis showed differences between characteristic pore indexes, like CPD and APD. Minerals additives to cement caused decrease from several to 50% of critical pore size and respectively average pore size related to reference concrete without SCM.
- A linear correlation between the  $D_{nssm}$  and CPD and APD for each concrete was found. The type of aggregate was found to influence on this relationship. The limestone aggregate being more sensitive for capillary pore index changes.

## ACKNOWLEDGEMENTS

The investigation was supported from European Funds – for the development of innovative economy: project POIG.01.01.02-24-005/09

## REFERENCES

1. Pedersen, K.H., Jensen, A.D., Skjřth-Rasmussen, M.S., Dam-Johansen, K., A review of the interference of carbon containing fly ash with air entrainment in concrete. *Progress in Energy and Combustion Science*, 34, 2008, 135–154
2. Pedersen, K.H., Jensen, A.D., Dam-Johansen, K., The effect of low-NOx combustion on residual carbon in fly ash and its adsorption capacity for air entrainment admixtures in concrete. *Combustion and Flame*, 157, 2010, 208–216
3. Kulaots, I., Hsu, A., Hurt, R.H., Suuberg, E.M., Adsorption of surfactants on unburned carbon in fly ash and development of a standardized foam index test. *Cement and Concrete Research*, 33, 2003, 2091–2099
4. Tsimas, S., Moutsatsou-Tsima, A., High-calcium fly ash as the fourth constituent in concrete: problems, solutions and perspectives. *Cement and Concrete Composites*, 27, 2005, 231–237

5. Antiohos, S., Papadakis, V.G., Maganari, K., Tsimas, S., The development of blended supplementary cementing materials consisting of high and low calcium fly ashes. Proceedings of the 11th International Congress on the Chemistry of Cement (ICCC), Durban, 2003
6. Bouzoubaa, N., Zhang, M.H., Malhotra, V.M., Mechanical properties and durability of concrete made with high-volume fly ash blended cements using a coarse fly ash. *Cement and Concrete Research*, 31, 2001, 1393–1402
7. Bentur, A., Impact of additions: indicators for durability and strength performance. International RILEM Workshop on Performance based Evaluation and Indicators for Concrete Durability, Madrid, 2006
8. Gibas, K., Glinicki, M.A., Nowowiejski, G., Evaluation of impermeability of concrete containing calcareous fly ash in respect to environmental media. *Roads and Bridges – Drogi i Mosty* 12, 2, 2013, 159-171
9. Wong, H.S., Pappas, A.M., Zimmerman, R.W., Buenfeld, N.R., Effect of entrained air voids on the microstructure and mass transport properties of concrete. *Cement and Concrete Research*, 41, 2011, 1067–1077
10. Tasong, W.A., Lynsdale, C.J., Cripps, J.C., Aggregate-cement paste interface Part I. Influence of aggregate geochemistry. *Cement and Concrete Research*, 29, 1999, 1019–1025
11. Dziuk, D., Giergiczny, Z., Garbacik, A., Calcareous fly ash as a main constituent of common cements. *Roads and Bridges – Drogi i Mosty*, 12, 1, 2013, 57-71
12. Yu, Z., Ye, G., The pore structure of cement paste blended with fly ash. *Construction and Building Materials*, 45, 2013, 30–35
13. Aponte, D.F., Barra, M., Vazquez, E., Durability and cementing efficiency of fly ash in concretes. *Construction and Building Materials*, 30, 2012, 537–546
14. Tang, L., Chloride transport in concrete – Measurement and prediction. Publication P-96:6, Chalmers University of Technology, Department of Building Materials, Göteborg, 1996
15. Yang, C.C., On the relationship between pore structure and chloride diffusivity from accelerated chloride migration test in cement-based materials. *Cement and Concrete Research*, 36, 2006, 1304–1311
16. Leemann, A., Loser, R., Münch, B., Influence of cement type on ITZ porosity and chloride resistance of self-compacting concrete. *Cement and Concrete Composites*, 32, 2010, 116-120